Supplementary Material (ESI) for CrystEngComm
This journal is © The Royal Society of Chemistry

Subtly tuning one N site of benzyl-1H-triazole ligands to build mono-nuclear subunits and tri-nuclear clusters to modify polyoxometalates

Ai-xiang Tian,* Ya-li Ning, Jun Ying,Guo-Cheng Liu, Xue Hou, Tian-jiao Li, Xiu-li Wang*

Department of Chemistry, Bohai University, Liaoning Province Silicon Materials Engineering Technology Research Centre, Jinzhou 121000, P. R. China

Table. S1. Selected Bond Lengths (Å) and Bond Angles (°) for Compounds **1**–**6**.

		Compound **1**	
Ag1-N1	2.150(5)	Ag1-N6	2.180(5)
Ag1-O6	2.698(4)	Ag1-O13	2.824(5)
Ag2-N4	2.144(5)	Ag2-N2	2.165(5)
N1-Ag1-N6	172.2(2)	N4-Ag2-N2	171.1(2)
		Compound **2**	
Ag1-N4	2.143(15)	Ag1-N3	2.207(14)
Ag1-O20	2.639(12)	Ag1-O13	2.898(11)
Ag2-N1	2.133(15)	Ag2-N5	2.202(16)
N4-Ag1-N3	169.7(6)	N1-Ag2-N5	170.4(7)
		Compound **3**	
Ag1-N10	2.125(14)	Ag1-N13	2.119(13)
Ag1-O19	2.662(9)	Ag2-N9	2.234(13)
Ag2-N11	2.243(13)	O34-Ag2	2.413(10)
O10-Ag2	2.666(10)	Ag4-N4	2.163(14)
Ag3-N7	2.115(13)	Ag5-N1	2.145(13)
Ag4-O18	2.568(12)	Ag5-O9	2.655(11)
Ag5-N5	2.154(11)	N14-K1	2.204(13)
Ag5-O21	2.828(10)	K1-O23	2.451(12)
N9-Ag2-N11	145.9(5)	N10-Ag1-N13	175.7(6)
N11-Ag2-O34	90.6(4)	N9-Ag2-O34	122.6(5)
N4-Ag4-N4	180	N7-Ag3-N7	180
N4-Ag4-O18	89.0(4)	N4-Ag4-O18	91.0(4)
O18-Ag4-O18	180	N1-Ag5-N5	171.1(5)
		Compound **4**	
Cu1-N1	1.971(9)	Cu1-N7	1.986(9)
Cu1-N4	2.003(9)	Cu1-N10	2.011(9)

∗ Corresponding author. Tel.: +86-416-3400158

E-mail address: tian@bhu.edu.cn (A.-X. Tian); wangxiuli@bhu.edu.cn (X.-L. Wang)

Cu1-O20	2.543(6)	Cu1-O23	2.584(6)
Cu2-N16	2.000(7)	Cu2-N13	2.013(8)
Cu2-O43	2.509(7)	Cu3-N28	1.990(8)
Cu3-N22	1.995(8)	Cu3-N19	2.003(9)
Cu3-N25	2.021(8)	Cu3-O51	2.496(6)
Cu3-O44	2.687(8)	Cu4-N40	1.979(9)
Cu4-N31	1.993(9)	Cu4-N34	2.007(8)
Cu4-N37	2.063(8)	Cu4-O12	2.534(8)
Cu4-O27	2.455(7)	Cu5-O24	2.505(8)
Cu5-N48	2.009(9)	Cu5-N44	1.996(8)
N7-Cu1-N10	85.7(3)	N1-Cu1-N7	170.3(4)
N16-Cu2-N16	180	N16-Cu2-N13	91.9(3)
N28-Cu3-N22	178.8(3)	N28-Cu3-N19	90.4(3)
N40-Cu4-N31	91.0(4)	N40-Cu4-N34	176.5(3)
N44-Cu5-N44	180	N44-Cu5-N48	91.6(3)
		Compound **5**	
O1W-Cu1	2.080(4)	Cu1-N2	1.976(4)
Cu1-N5	1.993(4)	Cu1-N8	2.112(4)
Cu1-N10	2.174(4)	O2W-Cu1	2.580(4)
Cu2-N7	2.021(4)	Cu2-N7	2.021(4)
Cu2-N11	2.082(5)	Cu2-N11	2.082(5)
Cu2-N4	2.354(5)	Cu2-N4	2.354(5)
N2-Cu1-N5	170.57(18)	N2-Cu1-O1W	85.34(17)
N7-Cu2-N7	180	N7-Cu2-N11	89.98(16)
		Compound **6**	
Cu1-N8	1.982(8)	Cu1-N2	2.000(8)
Cu1-N11	2.041(8)	Cu1-N6	2.037(8)
Cu1-O63	2.287(6)	O2W-Cu1	2.346(8)
Cu2-O63	1.962(6)	Cu2-N17	1.987(8)
Cu2-N1	1.998(8)	O1W-Cu2	1.984(6)
O13-Cu2	2.414(7)	Cu2-N7	2.528(7)
Cu3-O63	1.929(6)	Cu3-N14	1.977(7)
Cu3-N16	2.016(8)	Cu3-N10	2.041(8)
O19-Cu3	2.184(7)	O27-Cu4	2.337(6)
Cu4-N20	2.007(9)	Cu4-N22	2.047(8)
O63-Cu1-O2W	173.7(3)	N8-Cu1-N11	89.7(3)
O63-Cu2-O1W	173.5(3)	N17-Cu2-N1	174.9(4)
O63-Cu3-N16	87.4(3)	N14-Cu3-N10	91.1(3)
N20-Cu4-N20	180	N20-Cu4-N22	91.9(4)

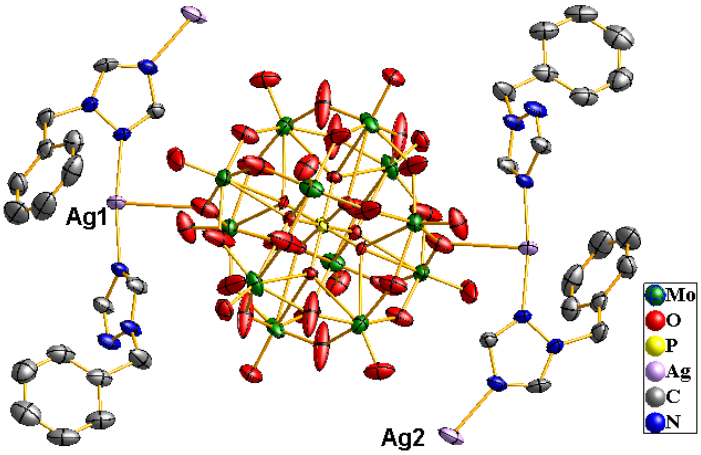

Fig. S1. ORTEP drawing of **1** with thermal ellipsoids at 50% probability. The H atoms have been omitted for clarity.

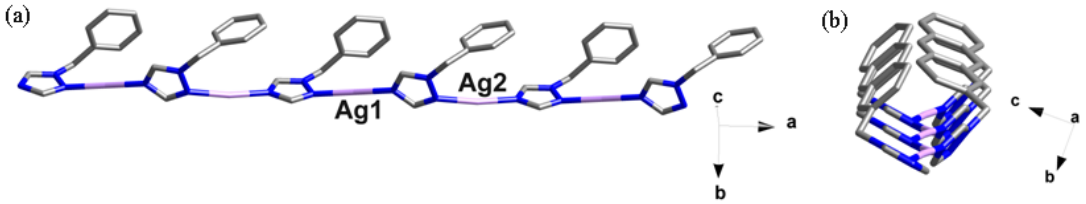

Fig. S2. The 1D metal-organic chain in compound **1** with a channel constructed by the twisted ligands.

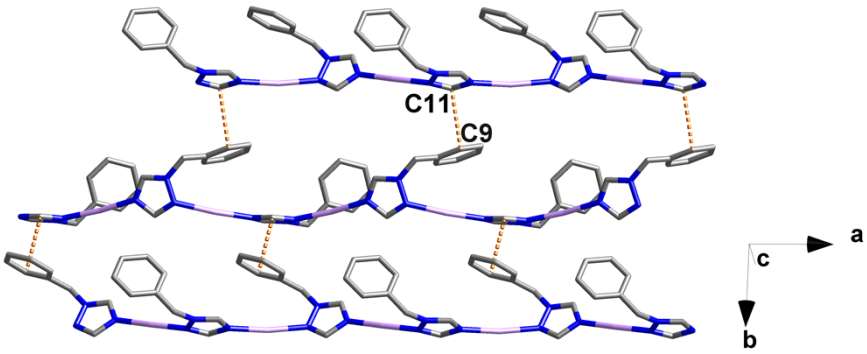

Fig. S3. The edge-to-face aromatic π…π stacking interactions of **1** between 2-btz molecules in adjacent Ag-(2-btz) chains (C9…C11 = 3.269 Å).

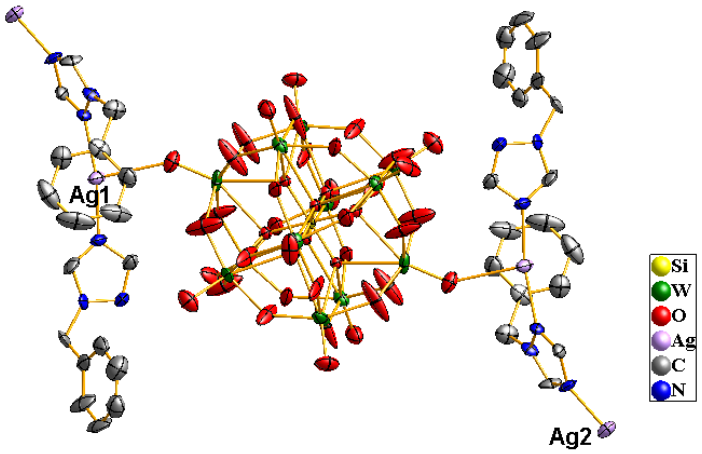

Fig. S4. ORTEP drawing of **2** with thermal ellipsoids at 50% probability. The H atoms have been omitted for clarity.

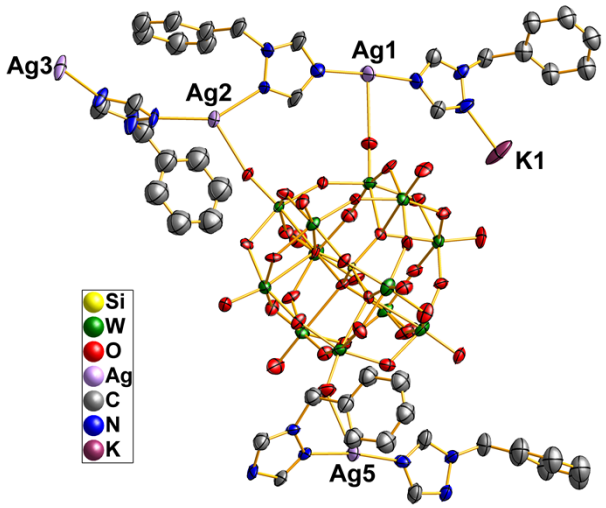

Fig. S5. ORTEP drawing of **3** with thermal ellipsoids at 50% probability. The H atoms have been omitted for clarity.

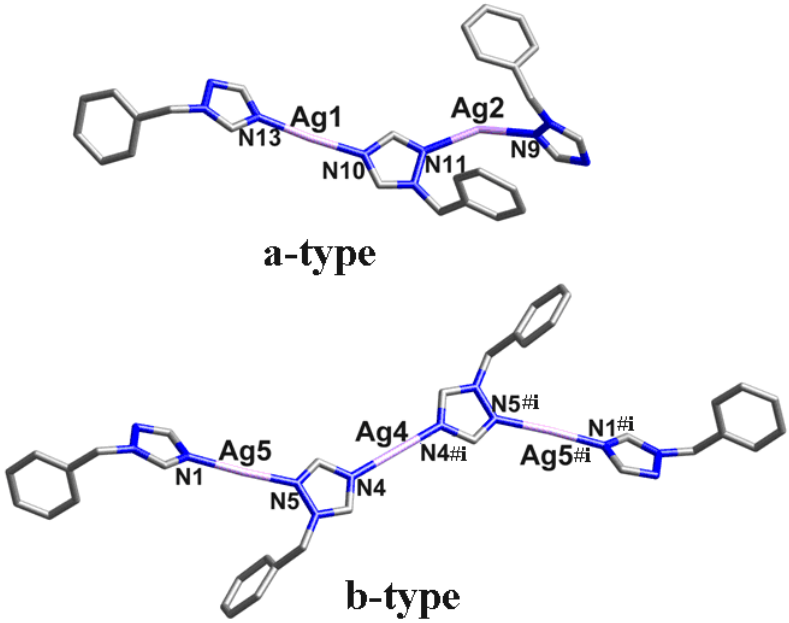

Fig. S6. Two types of Ag-(2-btz) subunits in compound **3** (Symmetry code #i: –x+1, –y+2, –z+1).

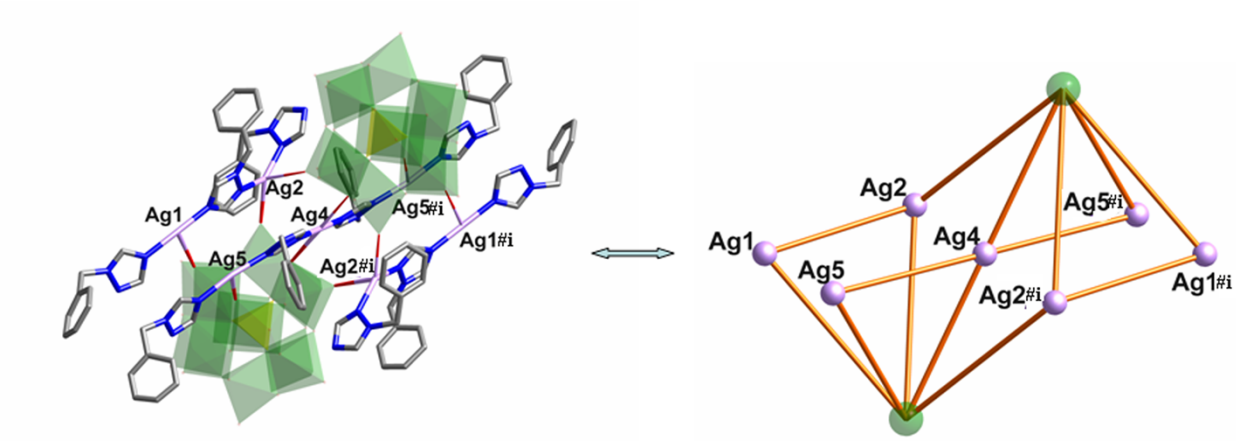

Fig. S7. Two SiW_{12} anions fused by Ag-(2-btz) subunits to construct an anion dimmer of **3** (Symmetry code #i: –x+1, –y+2, –z+1).

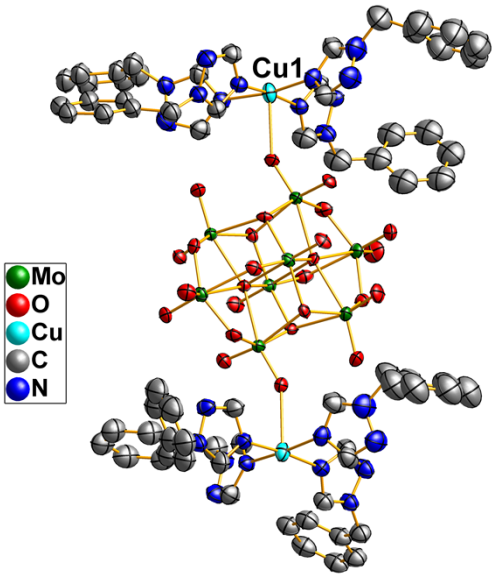

Fig. S8. ORTEP drawing of **4** with thermal ellipsoids at 50% probability. The H atoms have been omitted for clarity.

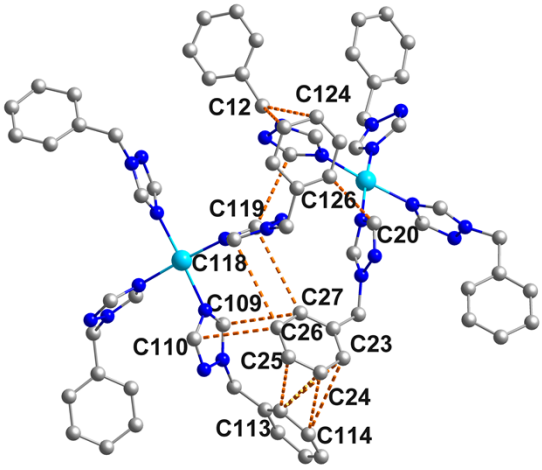

Fig. S9. The abundant aromatic π…π stacking interactions between 2-btz ligands to further stability the structure of compound **4**.

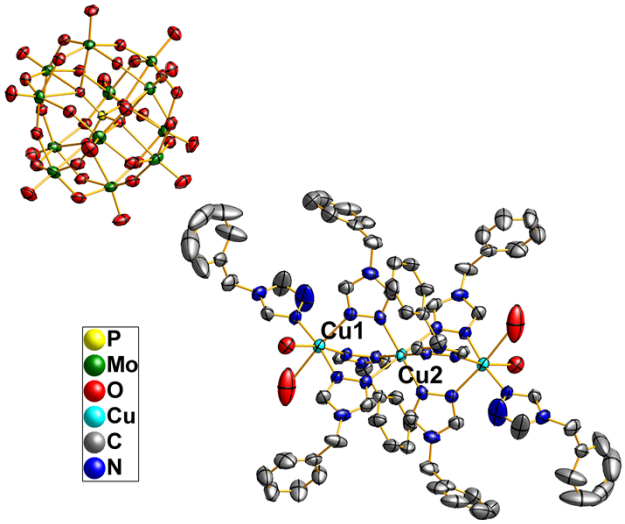

Fig. S10. ORTEP drawing of **5** with thermal ellipsoids at 50% probability. The H atoms have been omitted for clarity.

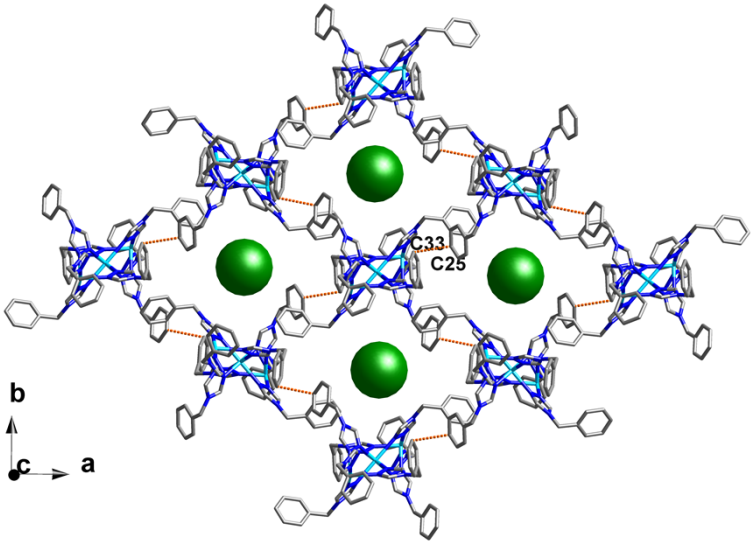

Fig. S11. The 2D supramolecular layer linked by aromatic π…π stacking interactions of compound **5** with anions (green) embedding in the grids.

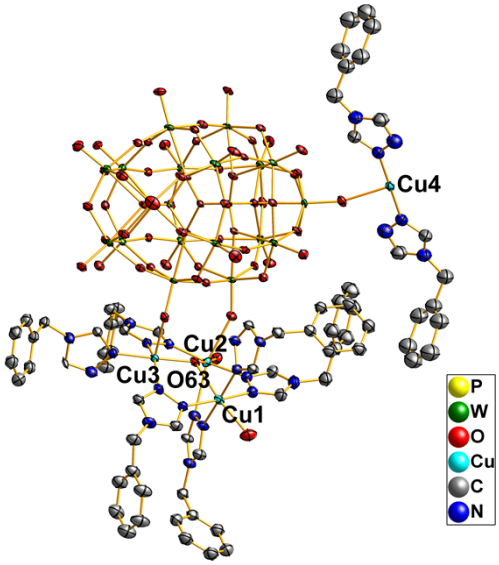

Fig. S12. ORTEP drawing of **6** with thermal ellipsoids at 50% probability. The H atoms have been omitted for clarity.

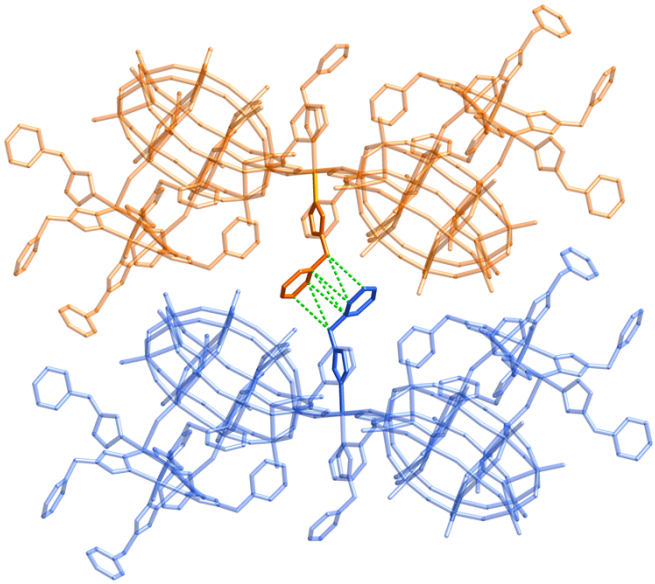

Fig. S13. The aromatic π…π stacking interactions (green dotted line) between dimers for stabilizing the structure of compound **6**.

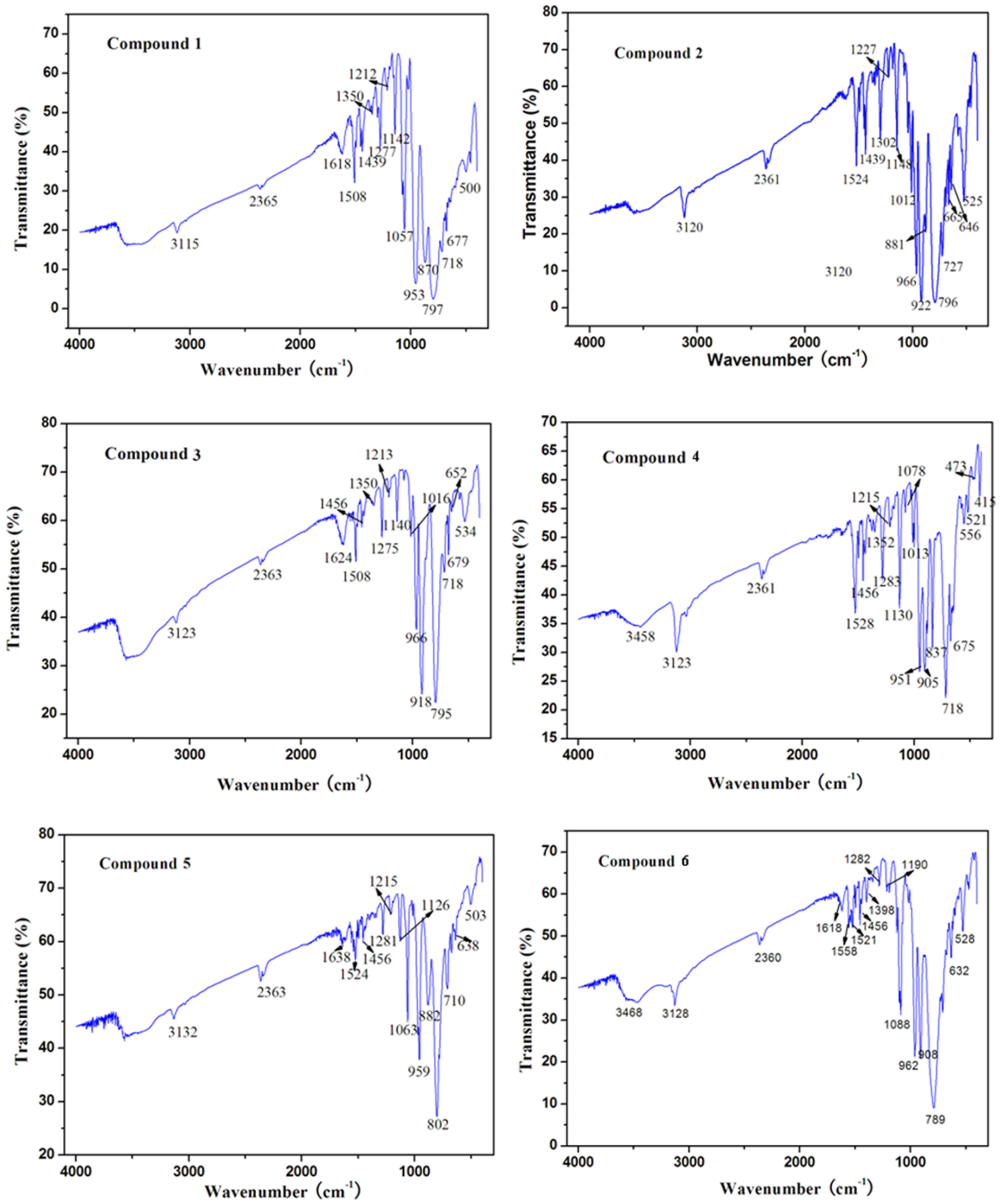

Fig. **S14.** The IR spectra of compounds **1**–**6**.

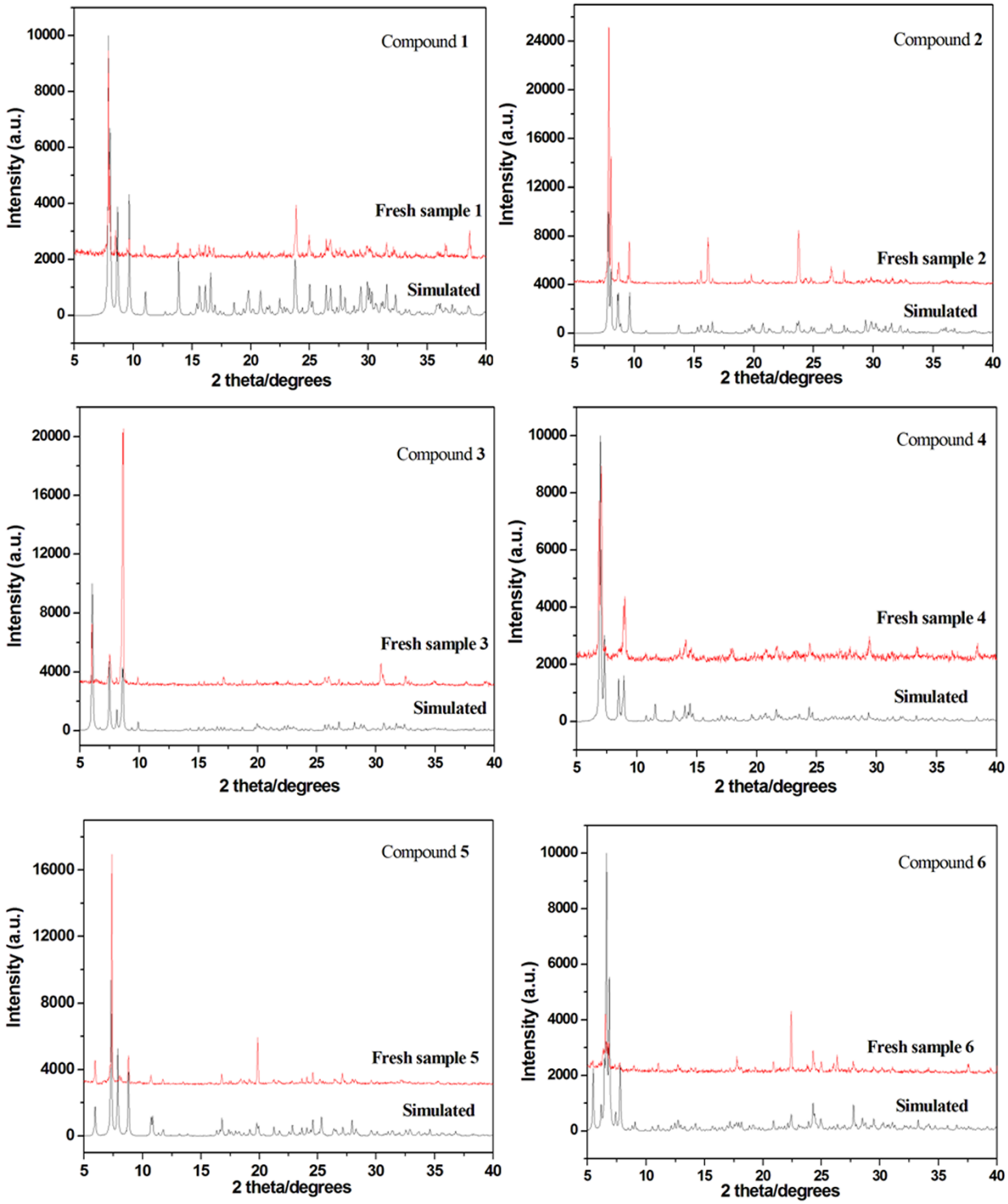

Fig. S15. The simulative (black line) and experimental (red line) powder X-ray diffraction patterns for compounds **1**–**6**.

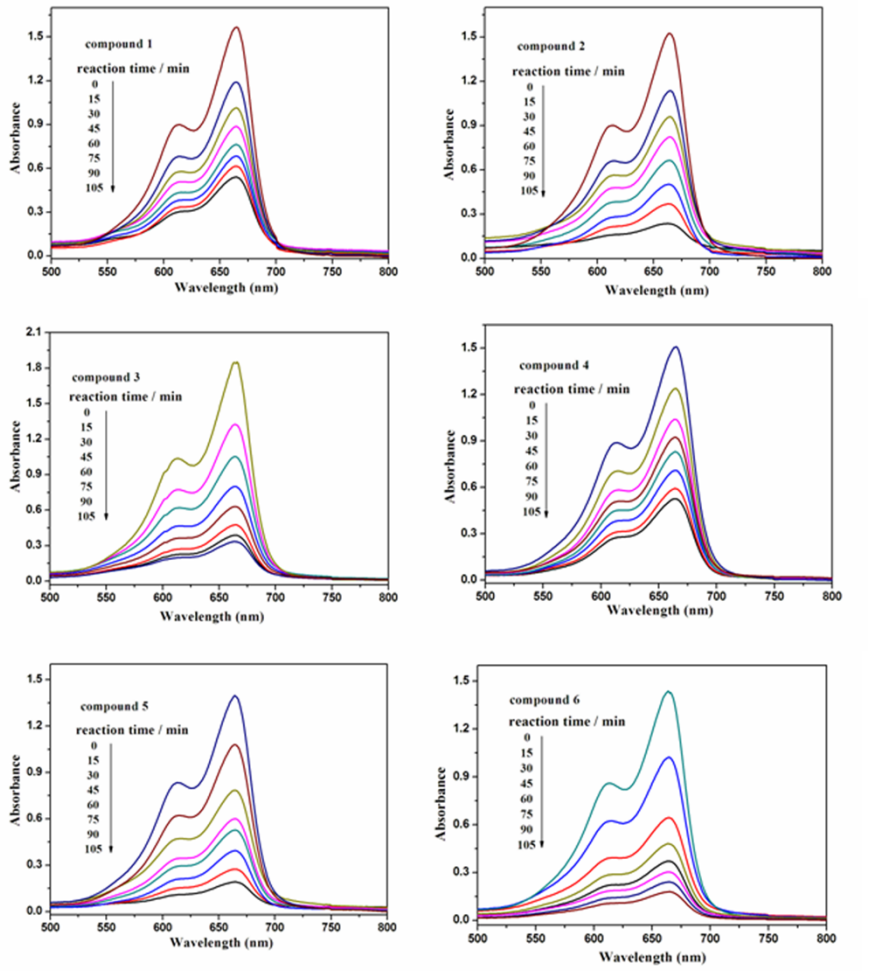

Fig. S16. Absorption spectra of the MB solution during the decomposition reaction under UV irradiation with the compounds **1**–**6** as catalyst.

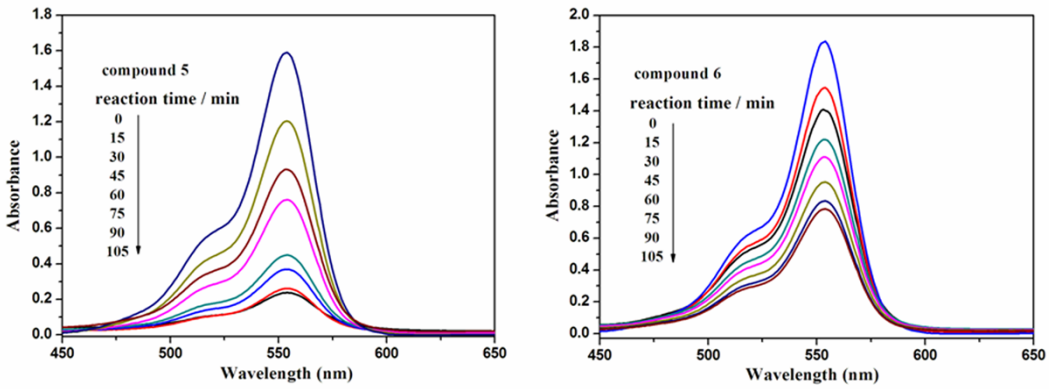

Fig. S17. Absorption spectra of the RhB solution during the decomposition reaction under UV irradiation with the compounds **5** and **6** as catalyst.

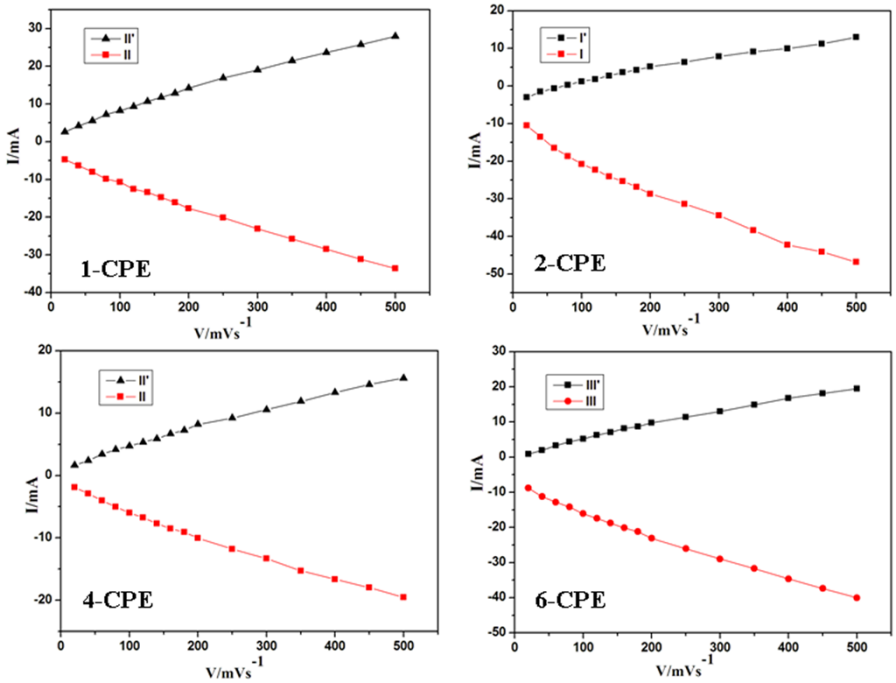

Fig. S18. The dependence of anodic peak and cathodic peak currents on scan rates of II-II' for **1**– and **4**–CPEs, I-I' for **2**–CPE and III-III' for **6**–CPE.

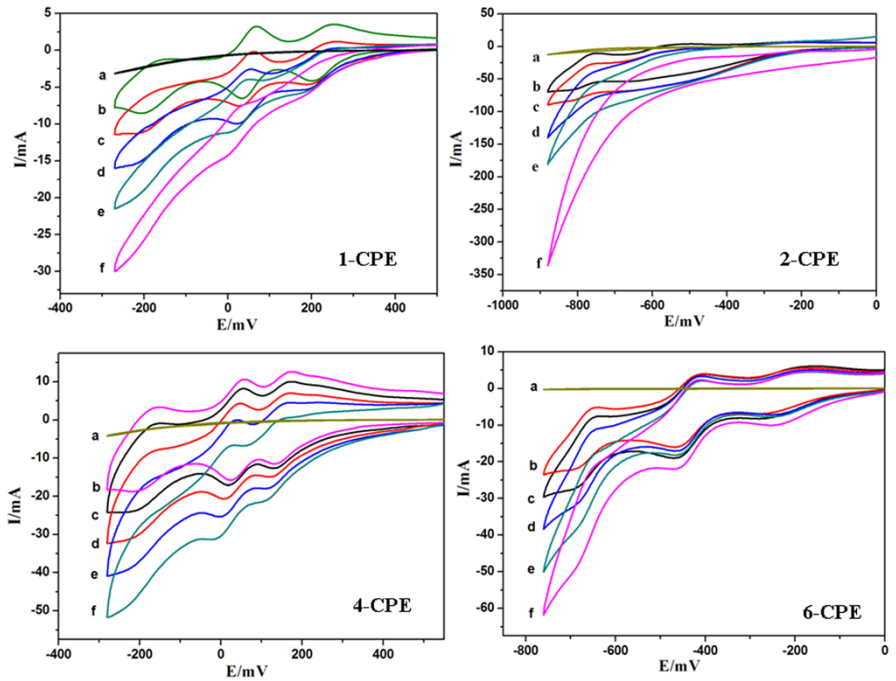

Fig. S19. Cyclic voltammograms of the **1**–, **2**–, **4**– and **6**–CPEs in 0.1 M H_2SO_4 + 0.5 M Na_2SO_4 aqueous solution containing 0(b); 2(c); 4(d); 6(e) and 8(f) mM $NaNO_2$ and a bare CPE (a) in a 4.0 mM $NaNO_2$ + 0.1 M H_2SO_4 + 0.5 M Na_2SO_4 solution. Scan rate: 200 mV·s^{-1}.

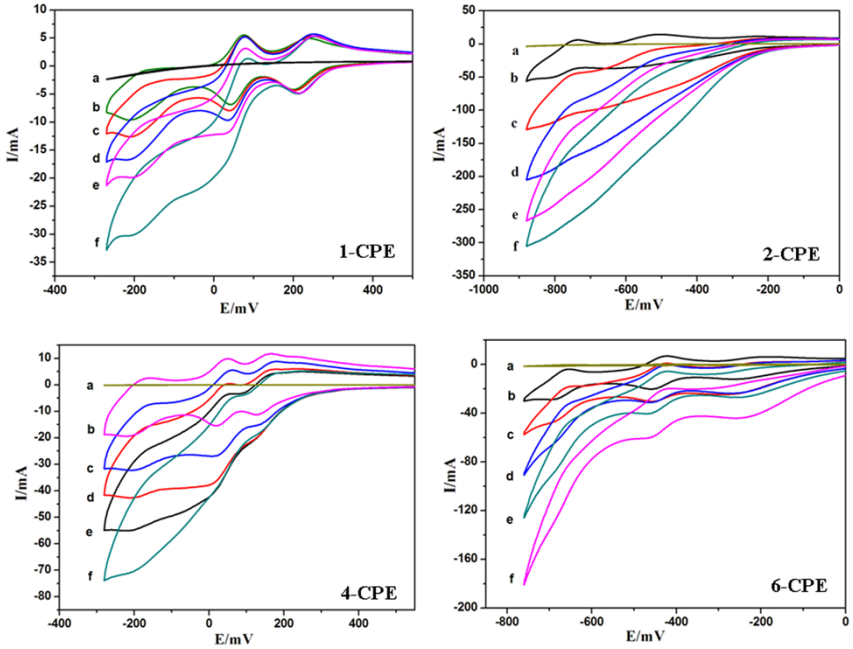

Fig. S20. Cyclic voltammograms of the **1**–, **2**–, **4**– and **6**–CPEs in 0.1 M H_2SO_4 + 0.5 M Na_2SO_4 aqueous solution containing 0(b); 2(c); 4(d); 6(e) and 8(f) mM H_2O_2 and a bare CPE (a) in a 4.0 mM H_2O_2 + 0.1 M H_2SO_4 + 0.5 M Na_2SO_4 solution. Scan rate: 200 mV·s^{-1}.

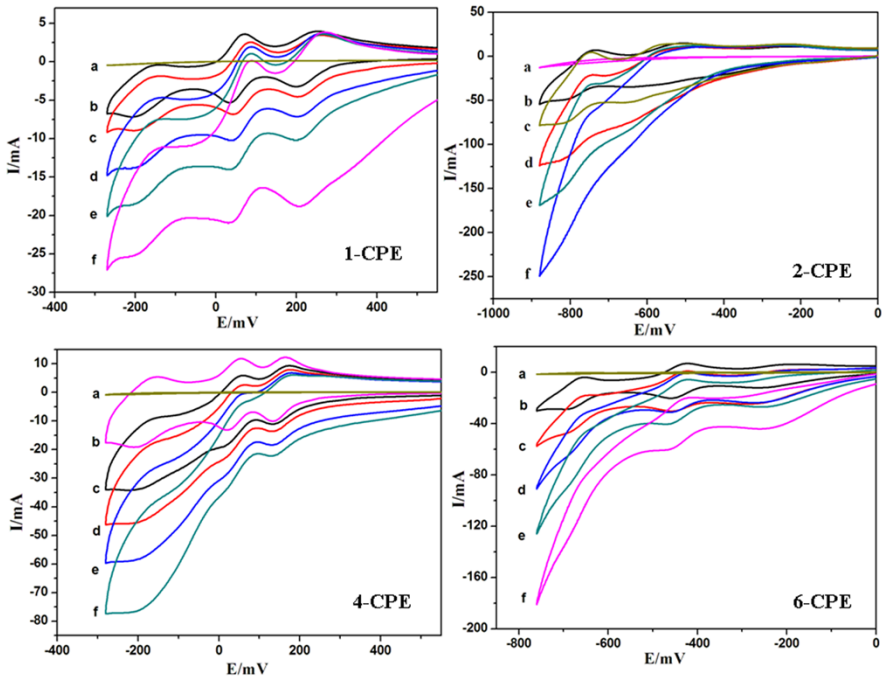

Figure. S21. Cyclic voltammograms of the **1**–, **4**–and **6**–CPEs in 0.1 M H_2SO_4 + 0.5 M Na_2SO_4 aqueous solution containing 0(b); 2(c); 4(d); 6(e) and 8(f) mM bromate and a bare CPE (a) in a 4.0 mM bromate + 0.1 M H_2SO_4 + 0.5 M Na_2SO_4 solution. Scan rate: 200 mV·s^{-1}.